

Black Magic in Gray Titania: Noble-Metal-Free Photocatalytic H₂ Evolution from Hydrogenated Anatase

Ning Liu¹, Xuemei Zhou¹, Nhat Truong Nguyen¹, Kristina Peters², Christopher Schneider¹, Detlef Freitag³, Dina Fattakhova-Rohlfing², Patrik Schmuki^{1,4}*

¹*Department of Materials Science WW-4, LKO, University of Erlangen-Nuremberg, Martensstrasse 7, 91058 Erlangen, Germany;*

²*Department of Chemistry and Center for NanoScience (CeNS), Ludwig-Maximilians-Universität München, Butenandtstr. 5-11 (Haus E), 81377 Munich, Germany;*

³*High Pressure Laboratory, Chair of Separation Science and Technology, University of Erlangen-Nuernberg, Haberstrasse 11, 91058 Erlangen, Germany;*

⁴*Department of Chemistry, King Abdulaziz University, Jeddah, Saudi Arabia.*

**Corresponding author. Tel.: +49 91318517575, fax: +49 9131 852 7582*

Email: schmuki@ww.uni-erlangen.de

Link to the published article:

<https://onlinelibrary.wiley.com/doi/full/10.1002/cssc.201601264>

'Black' TiO₂ has gained increasing interest because of its outstanding properties and promising applications in a wide range of fields. Among the outstanding features of the material is that certain synthesis processes lead to the formation of an intrinsic co-catalytic center and thus enable noble-metal free photocatalytic H₂ generation. In this work, we report 'grey TiO₂' by an appropriate hydrogenation treatment exhibits excellent photocatalytic hydrogen. In this case, by the employment of thermally stable and high-surface-area TiO₂ nanoparticles as well as mesoporous particles as the hydrogenation precursor, the appropriate extent of reduction of TiO₂ (coloration) and the formation of Ti³⁺ is the key for the efficient noble-metal-free photocatalytic H₂ generation. The EPR results reveal that 'grey TiO₂' shows stronger Ti³⁺ feature at $g \approx 1.93$ than 'black TiO₂' contributing to the intrinsic catalytic center for H₂ evolution.

Ever since Fujishima and Honda used TiO₂ as a photoanode in a photoelectrochemical cell (PEC) for hydrogen production [1], TiO₂ remains the most commonly used wide-band gap semiconductor photoanode for water splitting. The main reasons are that the material provides suitable band-edge positions relative to the water red-ox potentials, low cost, and a very high photocorrosion resistance [2-4].

However, the main weaknesses of TiO₂ are its large band gap (3.0-3.2 eV) and a very sluggish transfer kinetics of the charge carriers to the surrounding media. To achieve higher light conversion a broad range of approaches has been explored to narrow the TiO₂ optical band gap – such band gap engineering approaches have been based on the introduction of suitable energy states into the TiO₂ gap using doping elements (such as N, C, Cr or W) [4, 5]. To improve the slow electron transfer kinetics of TiO₂ to the adsorbed hydrogen species, the common remedy

for accelerating the H₂ generation is decorating the TiO₂ particles with co-catalyst particles, typically Pt, Au or Pd etc. that catalyze charge separation and hydrogen evolution [6, 7].

In the context of achieving a broad visible light absorption, a remarkable finding was reported in 2011 when Chen and Mao introduced so-called ‘black titania’ [8]. The material showed in optical absorption measurements a band gap of 1.54 eV, and after decoration with Pt as co-catalyst, a remarkably high water splitting performance [8]. This ‘black’ modification of TiO₂ was produced by exposing anatase nanoparticles to a high pressure/high temperature treatment in H₂ (HPH). Recently, we used this HPH treatment on TiO₂ nanotube arrays and commercial anatase particles and found another compelling feature of this material, which is that these modified structures provide a high and stable open-circuit photocatalytic hydrogen production rate without the presence of any noble-metal co-catalyst [9, 10]. Based on EPR and PL measurements we ascribed the intrinsic co-catalytic activation of anatase TiO₂ to specific defect centers formed during hydrogenation.

Despite these achievements, it still remains unclear whether the more coloration of TiO₂ (larger solar absorption) means more efficient for the photocatalytic activities. Moreover, the performance of ‘black TiO₂’ was reported different depending on different hydrogenation methods [16-19]. Hence a clear assessment of the key factors in the treatment to the enhanced photoactivities must be explored.

In the present work, anatase nanoparticles with different hydrogenation treatment (different temperature, flow and high pressure H₂ atmosphere) show significantly different photocatalytic activity for noble-metal-free H₂ generation. It shows that an appropriate hydrogenation treatment can lead to ‘grey TiO₂’ with more activation for noble-metal-free H₂ generation than ‘black TiO₂’, even the ‘black TiO₂’ shows much stronger solar absorption. Moreover EPR result for ‘grey TiO₂’ shows stronger Ti³⁺ peak ascribed the intrinsic co-catalytic activation than ‘black TiO₂’.

Hydrogenated TiO₂ nanoparticles were obtained by annealing pristine anatase TiO₂ nanoparticles (25 nm, Sigma-Aldrich) under H₂ flow and 20 bar at different temperature ranging 400-700 °C for 1 h using the flow furnace and the autoclave for high pressure (for details, see the Supporting Information).

To assess the ability of the different hydrogenated particles to produce photocatalytic H₂ without using any co-catalyst, we irradiated the particles under open circuit voltage (OCV) conditions in an aqueous methanol solution (50 vol %) under AM 1.5 (100 mW/cm²) solar simulator conditions (Fig. 1a). It can be seen that the hydrogenated particle show a significant photocatalytic H₂ evolution activity. As reference for a classic activation treatment for TiO₂, we include results for high pressure annealing in H₂ (HPH). The best result from the particles treated at 500 °C in flow H₂ is as efficient as the classic HPH result for noble-metal-free H₂ evolution. Nevertheless, the particles treated at higher temperature decay the efficiency gradually. The non-treated anatase does not produce any considerable amount of H₂.

The different hydrogenation treatment leads to different coloration of the particles and considerable absorption in the visible spectral range (see Fig. 1b). It can be seen for the photographs in Fig. 1b that the sample treated at 400 °C still maintains white color as the pristine TiO₂. The particles treated at 500 °C can be observed slightly grey color while the color of sample changes to more black after 600 °C hydrogenation and ‘black’ (black blue) TiO₂ was obtained at 700 °C. Fig. 1b shows the absorption in the visible light region gradually increased with the hydrogenation temperature in UV-vis absorption spectra. Absorption can be observed up to 800 nm. The particles treated at 700 °C provide the strongest absorption. The bandgap energy of the hydrogenated TiO₂ samples becomes lower with the increasing heating temperature, which is obtained on the basis of the Kubelka-Munk function in Fig. 1c.

These findings indicate that the magnitude in optical absorption (in the visible or UV range) does not correlate with the observed open-circuit photocatalytic H₂ production activity in Fig.

1a. Clearly, 'grey TiO₂' under OCV condition shows a significant more amount of photocatalytic H₂ production than 'black TiO₂'. Even more, the 'black' particles treated at 700 °C shows the lowest efficiency for noble-metal-free water splitting with the narrowest band-gap in Fig. 1c.

The X-ray diffraction (XRD) patterns of all the samples before and after hydrogenation treatments in Fig. 2a. The samples treated at the elevated temperature hydrogenation (500 and 600 °C) show pure anatase phase as the pristine anatase. The particles with the 700 °C hydrogenation show a major anatase phase with a small amount of rutile phase. Notably, the peak intensity of anatase significantly decreased after hydrogenation, which is in line with our finding for HPH samples with Rietveld refinement analysis [10]. The average crystallite size (using the Scherrer equation calculated) of the hydrogenated is appx. 20 nm, which is smaller than that of pristine powder (30 nm).

Further Raman spectra were acquired to investigate the structural changes of TiO₂ after hydrogenation in Fig. 2b. After hydrogenation, Raman bands at the main effect is a mild blue shift, evident e.g. at the main E_g peak, that is at 134 cm⁻¹ for the pristine powders to 144 cm⁻¹ for the hydrogenated powders. These observations are in line with models that indicate phonon confinement by a decrease of the effective particle size. Such a reduction of crystallite size could be due to amorphization of the original lattice induced by the H₂, if for instance as observed in literature [8, 12] the amorphous shell around the particles would increase. However, our TEM of the hydrogenated particles at different temperature did not show a significant increase of the thickness of these amorphous shells (Fig. 2c-g). TEM images for the sample at 700 °C hydrogenation shows an aggregation in the nanoparticle morphology. Moreover, from XPS (in Fig. 2d) no significant variation in the composition, such as Ti³⁺, of the samples before and after hydrogenation could be observed.

In order to gain additional information on the electronic nature of the defect structure, electron paramagnetic resonance (EPR) measurements were carried out. From EPR spectra taken for different samples at 80 K in dark, a different defect signature becomes apparent (Fig. 3). All the samples, except the sample treated at 700 °C show the peaks with a g-factor of 2.003 which in the literature [13] are typically assigned to oxygen vacancies (OV). The ‘grey’ samples show the presence of a EPR signal of g-value of 1.91 as paramagnetic defect in the dark conditions. The feature has been ascribed to a Ti^{3+} species existing in the subsurface of TiO_2 [9, 10], contributing to the intrinsic catalytic center for H_2 evolution. Moreover, the sample treated at 500 °C shows much stronger signals at g-value of 1.91 and 2.003 than that for the sample treated at 600 °C which is in line with the co-catalytic activity for H_2 evolution. Interestingly, ‘black TiO_2 ’ shows a very high intensity peak at 1.957, which reveals the amount of Ti^{3+} species in the bulk [14, 15]. Combined with water splitting results, the high concentration of Ti^{3+} species in ‘black TiO_2 ’ leads to the severe bulk defects, which act as charge recombination centers.

Additionally, the photocatalytic performance of TiO_2 for water splitting application depends, as any surface controlled reaction directly on the number of accessible active surface sites. The 3D-titania mesoporous structures feature high accessible surface areas in combination with the interconnected network of a bulk titania phase [11, 12]. Thus we also investigate the noble-metal-free water splitting behavior of mesoporous TiO_2 with large surface area (approx. 130 m^2/g , compared with the surface area of TiO_2 nanoparticles 50 m^2/g , SI), confined porous structure and high surface to volume ratio by different hydrogenation treatments. Fig. 4a and b show the TEM images of mesoporous anatase with dense pore walls, being composed of sintered, interconnected nanoparticles of particle size of approx. 8 nm. After typical hydrogenation leads to ‘grey TiO_2 ’, the size of the crystalline domains increased from 8 nm to 13.6 in Fig. 4c and d. Additionally, for both samples, HRTEM cannot obviously reveal the presence of amorphous regions. Fig. 4e shows the amount of H_2 produced under open-circuit

conditions from the 'grey TiO₂' and 'black TiO₂' (as shown in photograph in Fig. 4e) of mesoporous structure comparing with that of 'grey TiO₂' of nanoparticles. In the mesoporous case, the 'grey TiO₂' shows the higher H₂ evolution than 'black TiO₂' as expected. Moreover, the mesoporous 'grey TiO₂' shows about 2 times higher H₂ evolution rate than 'grey' nanoparticles because of the larger surface area.

In summary, in the present work, we investigated 'grey TiO₂' and 'black TiO₂' resulting from different hydrogenation of nanostructure and mesoporous structure and their efficiency towards photocatalytic H₂ evolution. The results show that photocatalytic efficiency for noble-metal-free H₂ evolution is not related to the coloration of TiO₂ by different hydrogenation reduction. The 'grey TiO₂' shows stronger Ti³⁺ feature at $g \approx 1.93$ contributing to the intrinsic catalytic center in hydrogenated materials for H₂ evolution. The 'black TiO₂' treated at higher temperature shows highly concentrated bulk defects at $g \approx 1.96$ of EPR results, which act as the recombination centers inhibiting the photoactivities. The temperature for hydrogenation is the determining factor for the photocatalytic activity for noble-metal-free water splitting both in flow and high pressure cases.

References:

- [1] A. Fujishima, K. Honda, *Nature*, 1972, 238, 37.
- [2] A. Fujishima, X. Zhang, D.A. Tryk, *Surf. Sci. Rep.*, 2008, 63, 515.
- [3] U. Diebold, *Surf. Sci. Rep.*, 2003, 48, 53.
- [4] P. Roy, S. Berger, P. Schmuki, *Angew. Chem. Int. Ed.*, 2011, 50, 2904.
- [5] I. Paramasivam, H. Jha, N. Liu, P. Schmuki, *Small*, 2012, 8, 3073.
- [6] K. Connelly, A. K. Wahab, H. Idriss, *Mater Renew Sustain Energy*, 2012, 1, 3.

- [7] M. Ni, M. K. H. Leung, D. Y. C. Leung, K. Sumathy, *Renewable and Sustainable Energy Reviews*, 2007, 11, 401-425.
- [8] X. Chen, L. Liu, P. Y. Yu, S. S. Mao, *Science*, 2011, 331, 746.
- [9] N. Liu, C. Schneider, D. Freitag, M. Hartmann, U. Venkatesan, J. Müller, E. Spiecker, Schmuki P., *Nano Lett.*, 2014, 14 , 3309.
- [10] N. Liu, C. Schneider, D. Freitag, U. Venkatesan, V. R. R. Marthala, M. Hartmann, B. Winter, E. Spiecker, A. Osvet, E. M. Zolnhofer, K. Meyer, T. Nakajima, X. Zhou, P. Schmuki, *Angew. Chem. Int. Ed.*, 2014, 126, 14425.
- [11] Szeifert, J. M.; Feckl, J. M.; Fattakhova-Rohlfing, D.; Liu, Y. J.; Kalousek, V.; Rathousky, J.; Bein, T. *J. Am. Chem. Soc.* 2010, 132, 12605
- [12] W. Zhou, W. Li, J.-Q. Wang, Y. Qu, Y. Yang, Y. Xie, K. Zhang, L. Wang, H. Fu, D. Zhao, *J. Am. Chem. Soc.* 2014, 136, 9280–9283.
- [13] H. Liu, H. T. Ma, X. Z. Li, W. Z. Li, M. Wu, X. H. Bao, *Chemosphere*, 2003, 50, 39
- [14] M. Chiesa, M. C. Paganini, S. Livraghi and E. Giamello, *Phys. Chem. Chem. Phys.*, 2013, 15, 9435.
- [15] L. B. Xiong, J. L. Li, B. Yang and Y. Yu, *J. Nanomater.*, 2012, 2012, 13.
- [16] Wang G., Wang H., Ling Y., Tang Y., Yang X., Fitzmorris R. C., Wang C., Zhang J. Z., Li Y., *Nano Lett.* 2011, 11, 3026.
- [17] Lu X., Wang G., Zhai T., Yu M., Gan J., Tong Y., Li Yat, *Nano Lett.* 2012, 12, 1690.
- [18] Naldoni A., Allieta M., Santangelo S., Marelli M., Fabbri F., Cappelli S., Bianchi C. L., Psaro R., Santo V. D., *J. Am. Chem. Soc.*, 2012, 134, 7600.

[19] Zheng Z., Huang B., Lu J., Wang Z., Qin X., Zhang X., Dai Y., Whangbo M., Chem. Commun. 2012, 48, 5733.

Figure captions:

Fig. 1 (a) Photocatalytic hydrogen evolution rate from TiO₂ nanoparticles with different hydrogenation treatments under AM 1.5 (100 mW/cm²) illumination; (b) Integrated light reflectance results of TiO₂ with different hydrogenation treatments with corresponding photographs of the powders; (c) The plot of the transformed Kubella-Munk function vs. the gap energy of the TiO₂ samples.

Fig. 2 (a) The X-ray diffraction patterns and (b) Raman spectra of TiO₂ before and after hydrogenation; (c) TEM images and (d) XPS of TiO₂ nanoparticles before and after hydrogenation .

Fig. 3 EPR spectra for TiO₂ nanoparticles with different hydrogenation treatments at 80 K in dark.

Fig. 4 TEM images of mesoporous TiO₂ (a+b) and hydrogenated TiO₂ (c+d) showing the crystalline pore walls assembled from nanocrystals. The inset in (a) and (d) shows the corresponding selected area electron diffraction (SAED) pattern, which is in a good agreement with the TiO₂ anatase structure; (e) Photocatalytic hydrogen evolution rate from TiO₂ mesoporous materials with different treatments compared with 'grey TiO₂' under AM 1.5 (100 mW/cm²) illumination.

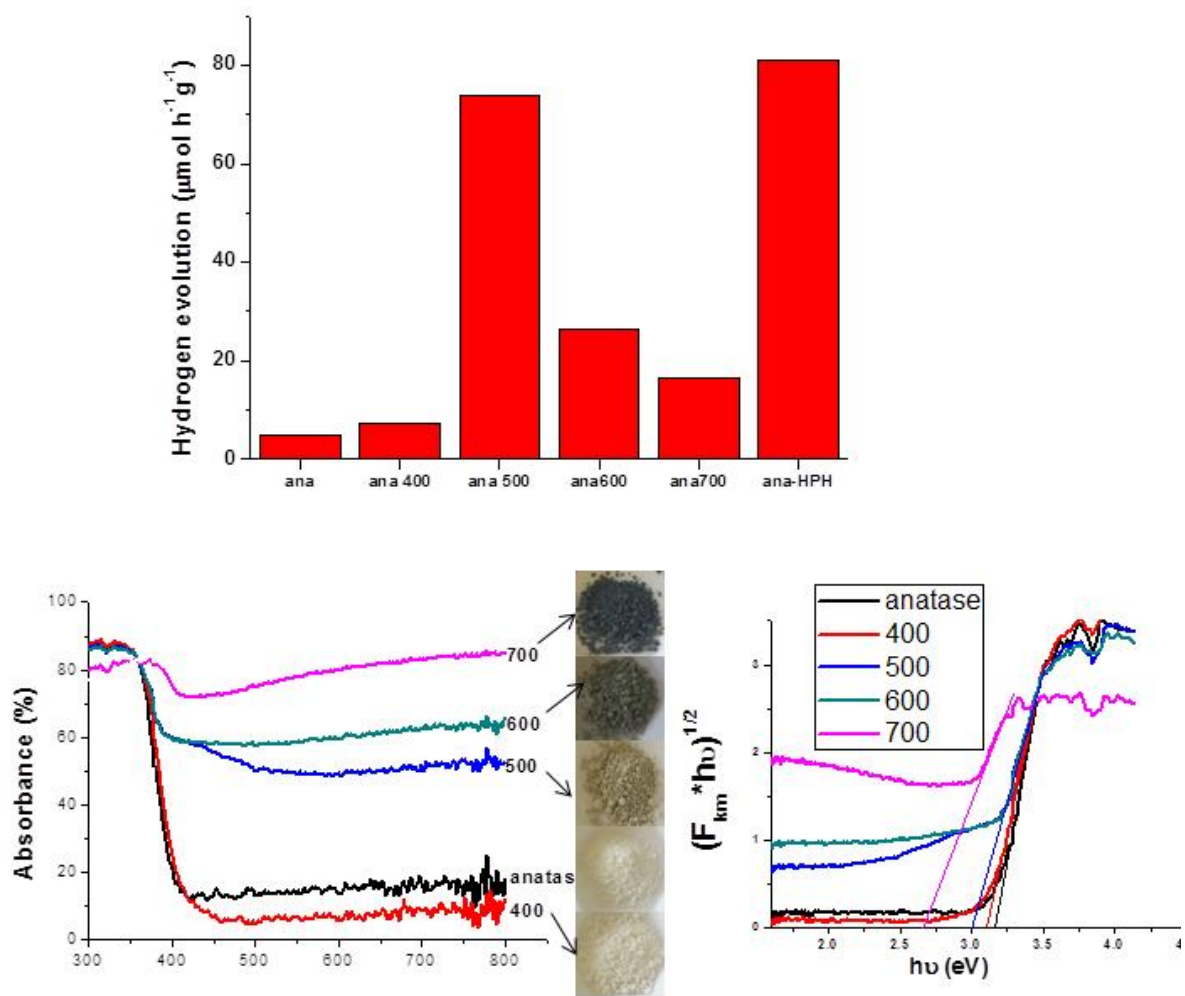
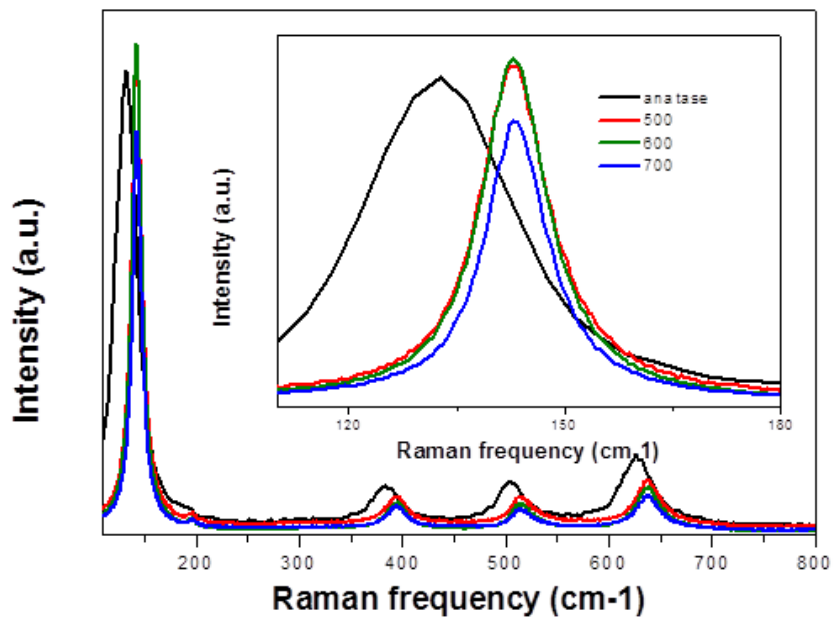
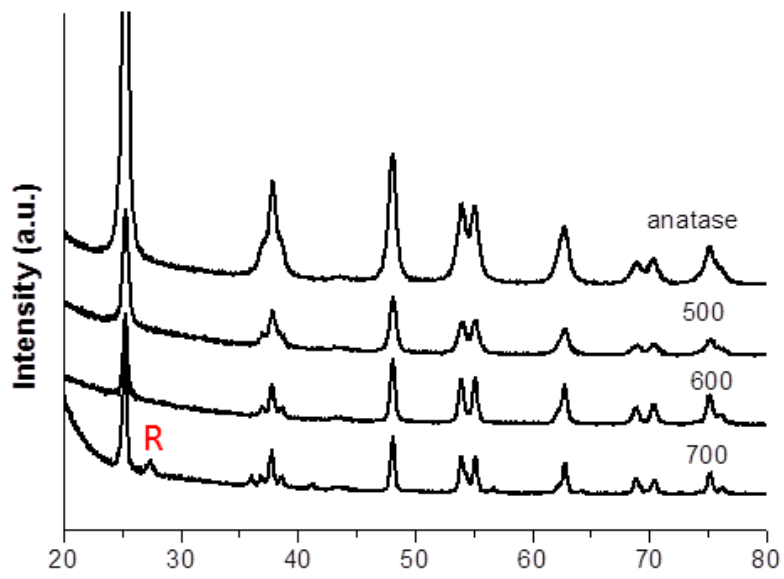
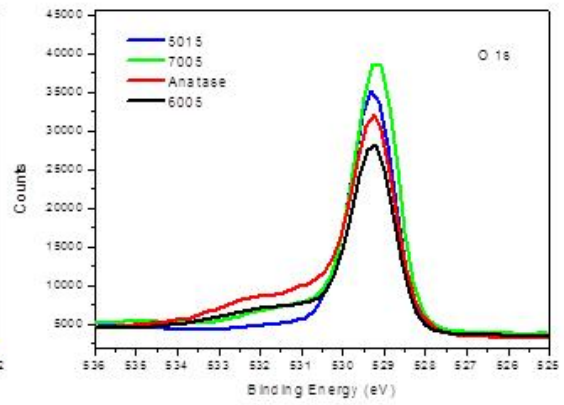
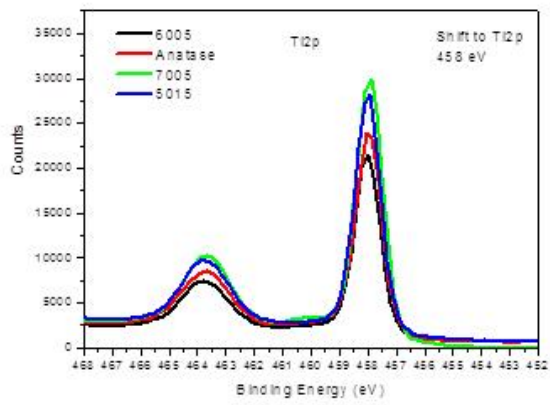
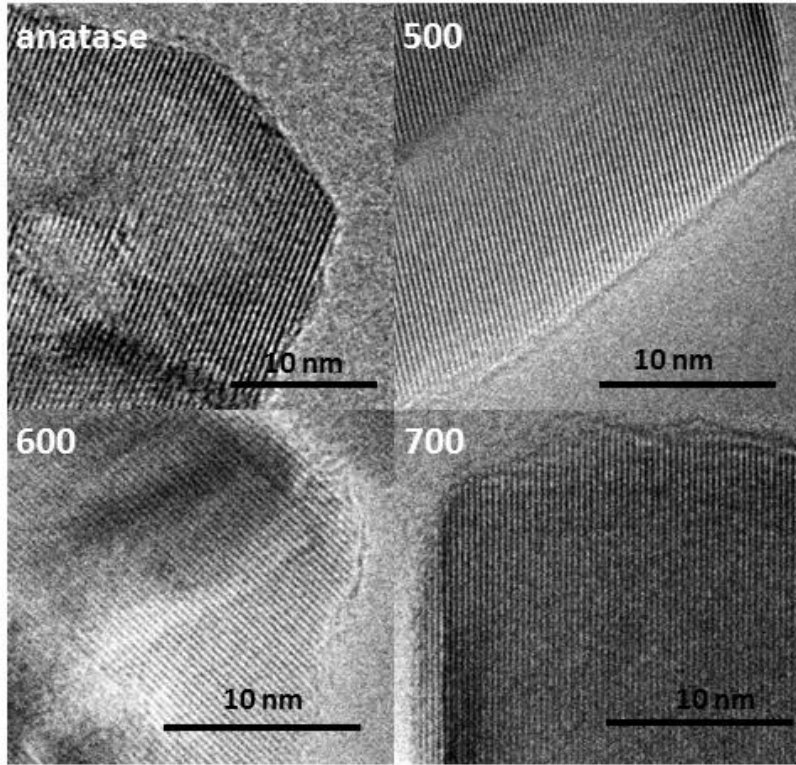


Fig. 1





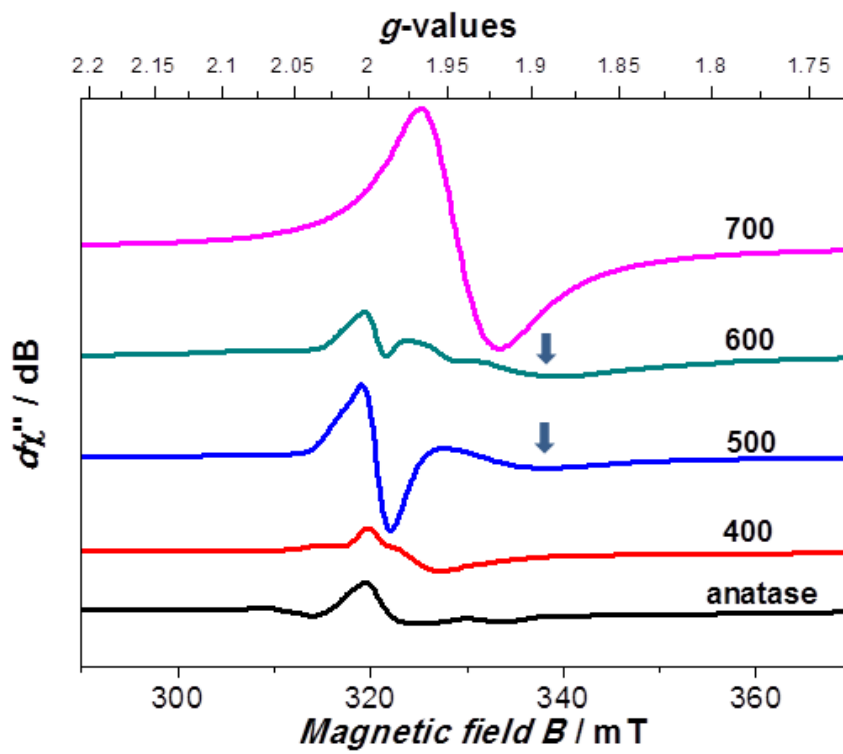


Fig. 3

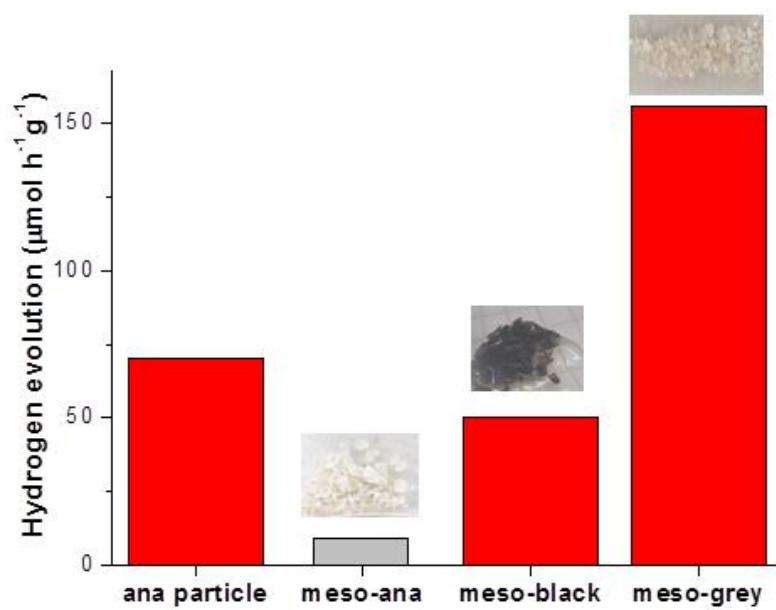
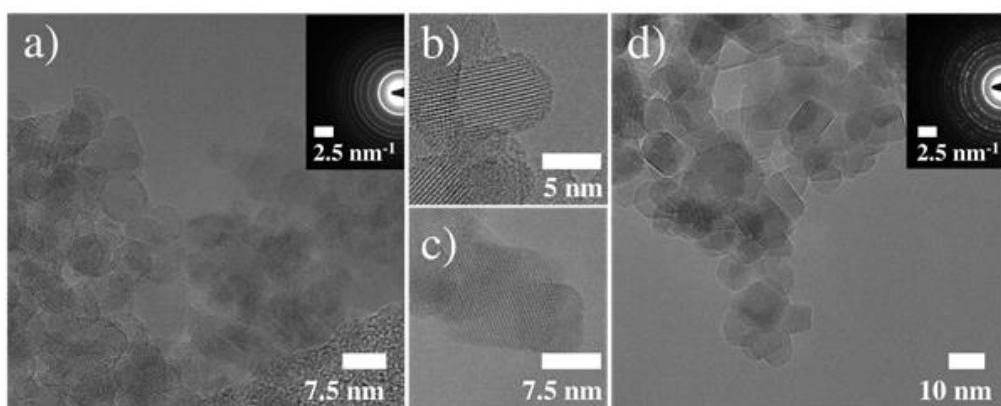


Fig. 4